Acta Crystallographica Section B
Structural Science
ISSN 0108-7681

Low-temperature structure of rubrene single crystals grown by vapor transport

Oana D. Jurchescu,* Auke Meetsma and Thomas T. M. Palstra

Solid State Chemistry Laboratory, Materials Science Centre, University of Groningen, Nijenborgh 4, 9747 AG Groningen, The Netherlands

Correspondence e-mail: o.d.jurchescu@rug.nl

Received 15 December 2005
Accepted 25 January 2006

We report the crystal structure of rubrene, $C_{42}H_{28}$ (5,6,11,12-tetraphenyltetracene), in the temperature interval 100–300 K. The crystals are grown by physical vapor transport in an open system. The crystal structure is orthorhombic over the entire temperature range.

1. Introduction

The electronic properties of polymers and molecular crystals are of great interest owing to fundamental questions on electron transport and associated applications. The present focus is in developing novel chemical structures, as well as improved fabrication techniques that are able to open new fields for electronic applications based on organic materials. A number of molecular conductors are of current interest. Rubrene (I) exhibits interesting physical properties, such as having one of the highest reported electronic mobilities at room temperature (Sundar *et al.*, 2004). Emerging new applications based on rubrene are organic field-effect transistors (OFETs; Sundar *et al.*, 2004; de Boer *et al.*, 2004; Podzorov *et al.*, 2004; Butko *et al.*, 2005) and organic light emitting diodes (OLEDs; Oyamada *et al.*, 2005; Li *et al.*, 2005).

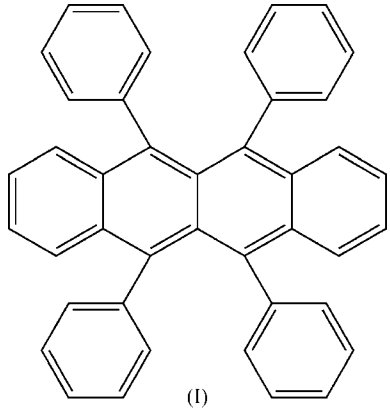

(I)

Although the technological development is relatively fast, fundamental questions concerning the intrinsic mechanism of conduction have still not been answered. Moreover, for the title compound, little attention has been paid to the interplay between its crystal structure and electronic properties. Interest in the present work is guided by intriguing changes which have been observed at low temperature in the mobility of field-effect transistors built on rubrene single crystals (de Boer *et al.*, 2004; Podzorov *et al.*, 2004).

Table 1
Experimental details.

	100 K	150 K	200 K	293 K
Crystal data				
Chemical formula	$C_{42}H_{28}$	$C_{42}H_{28}$	$C_{42}H_{28}$	$C_{42}H_{28}$
M_r	532.68	532.68	532.68	532.68
Cell setting, space group	Orthorhombic, *Cmca*	Orthorhombic, *Cmca*	Orthorhombic, *Cmca*	Orthorhombic, *Cmca*
Temperature (K)	100 (1)	150 (1)	200 (1)	293 (1)
a, b, c (Å)	26.789 (4), 7.170 (1), 14.211 (2)	26.775 (4), 7.1680 (10), 14.258 (2)	26.838 (4), 7.181 (1), 14.332 (2)	26.86 (1), 7.193 (3), 14.433 (5)
V (Å^3)	2729.6 (7)	2736.4 (7)	2762.1 (7)	2788.5 (18)
Z	4	4	4	4
D_x (Mg m^{-3})	1.296	1.293	1.281	1.269
Radiation type	Mo $K\alpha$	Mo $K\alpha$	Mo $K\alpha$	Mo $K\alpha$
No. of reflections for cell parameters	4621	4648	4251	1924
θ range (°)	2.9–29.3	2.9–27.5	2.8–27.4	2.8–23.4
μ (mm^{-1})	0.07	0.07	0.07	0.07
Crystal form, color	Platelet, orange	Platelet, orange	Platelet, orange	Platelet, orange
Crystal size (mm)	0.51 × 0.45 × 0.03	0.51 × 0.45 × 0.03	0.51 × 0.45 × 0.03	0.51 × 0.45 × 0.03
Data collection				
Diffractometer	Bruker Smart Apex CCD area detector	Bruker Smart Apex CCD area detector	Bruker Smart Apex CCD area detector	Bruker Smart Apex CCD area detector
Data collection method	φ and ω scans	φ and ω scans	φ and ω scans	φ and ω scans
Absorption correction	Multi-scan	Multi-scan	Multi-scan	Multi-scan
T_{min}	0.952	0.974	0.956	0.949
T_{max}	0.998	0.998	0.996	0.998
No. of measured, independent and observed reflections	10 125, 1424, 1201	10 088, 1427, 1101	10 162, 1437, 1075	10 259, 1451, 938
Criterion for observed reflections	$I>2\sigma(I)$	$I>2\sigma(I)$	$I>2\sigma(I)$	$I>2\sigma(I)$
R_{int}	0.035	0.045	0.045	0.061
θ_{max} (°)	26.4	26.4	26.4	26.4
Range of h, k, l	$-31 \Rightarrow h \Rightarrow 33$ $-8 \Rightarrow k \Rightarrow 8$ $-17 \Rightarrow l \Rightarrow 17$	$-33 \Rightarrow h \Rightarrow 33$ $-8 \Rightarrow k \Rightarrow 8$ $-17 \Rightarrow l \Rightarrow 17$	$-33 \Rightarrow h \Rightarrow 28$ $-8 \Rightarrow k \Rightarrow 8$ $-17 \Rightarrow l \Rightarrow 17$	$-33 \Rightarrow h \Rightarrow 28$ $-8 \Rightarrow k \Rightarrow 8$ $-18 \Rightarrow l \Rightarrow 18$
Refinement				
Refinement on	F^2	F^2	F^2	F^2
$R[F^2>2(F^2)]$, $wR(F^2)$, S	0.037, 0.099, 1.06	0.039, 0.105, 1.04	0.041, 0.113, 1.03	0.044, 0.123, 1.03
No. of reflections	1424	1427	1437	1451
No. of parameters	124	124	124	124
H-atom treatment	Refined independently	Refined independently	Refined independently	Refined independently
Weighting scheme	$w = 1/[\sigma^2(F_o^2) + (0.0473P)^2 + 2.3678P]$, where $P = (F_o^2 + 2F_c^2)/3$	$w = 1/[\sigma^2(F_o^2) + (0.0526P)^2 + 1.7289P]$, where $P = (F_o^2 + 2F_c^2)/3$	$w = 1/[\sigma^2(F_o^2) + (0.0595P)^2 + 1.3599P]$, where $P = (F_o^2 + 2F_c^2)/3$	$w = 1/[\sigma^2(F_o^2) + (0.070P)^2 + 0.P]$, where $P = (F_o^2 + 2F_c^2)/3$
$(\Delta/\sigma)_{max}$	< 0.0001	< 0.0001	< 0.0001	< 0.0001
$\Delta\rho_{max}$, $\Delta\rho_{min}$ (e^{-3})	0.26, −0.21	0.25, −0.18	0.23, −0.18	0.15, −0.17

Computer programs used: *SMART* (Bruker, 2000), *SAINT* (Bruker, 2000), *XPREP* (Bruker, 2000), *SHELXS*97 (Sheldrick, 1997*a*), *SHELXL*97 (Sheldrick, 1997*b*), *PLATON* (Spek, 2003).

2. Experimental

In this study we investigate the structure of rubrene single crystals and correlate it with the electrical properties. The crystals are formed through competition between π-stacking and quadrupolar interactions. Owing to these weak interactions, different growth conditions can lead to different polymorphs. This feature is widely encountered for molecular crystals. Several polymorphs of rubrene have been reported. A monoclinic phase was described by Taylor (1936) and a triclinic polymorph was explored by Akopyan *et al.* (1962). Unfortunately, these reports do not mention the growth method. An orthorhombic form of rubrene (space group *Aba*2) was reported for crystals grown from vapor in a vacuum using sealed ampoules (Henn & Williams, 1971). For crystals obtained in a closed system, in a two-zone furnace, at ambient pressure, Bulgarovskaya *et al.* (1983) reported a second orthorhombic polymorph, with space group *Bbam*. For all the polymorphs investigated previously, only the room-temperature structure is reported, thus no relation with the physical properties at low temperature can be made.

Moreover, crystals grown by physical vapor transport in an inert gas, in an open system and continuous flow (Laudise *et al.*, 1998) are preferred for electronic applications, because they have the highest purity and thus the largest mobility. Still, no crystal structure determination is available for crystals obtained by this method. In this study we report the crystal structure between 100 and 300 K of rubrene single crystals

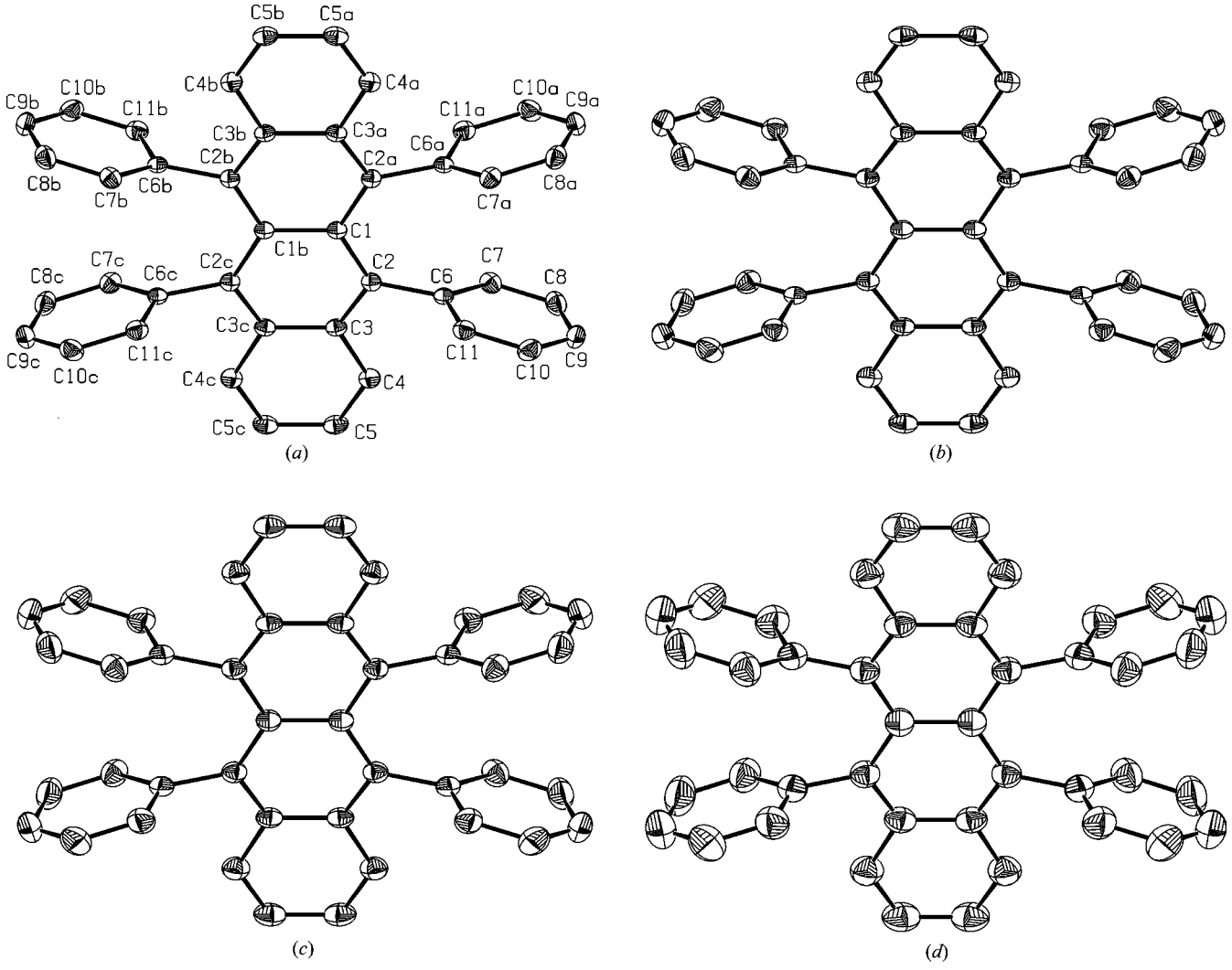

Figure 1
Perspective *ORTEP* (Spek, 2003) drawing of the rubrene molecule illustrating the conformation and the adopted labeling scheme for the non-H atoms at (*a*) 100 K, (*b*) 150, (*c*) 200 K and (*d*) room temperature. Displacement ellipsoids for non-H atoms are represented at the 50% probability level.

grown by physical vapor transport (PVT). This growth method yields orange crystals with orthorhombic symmetry, space group *Cmca*. We notice that the polymorph of the crystals grown with this method coincides[1] with that obtained for the crystals grown in sealed ampoules by Bulgarovskaya *et al.* (1983).

The rubrene single crystals investigated in this work were grown using physical vapor transport under a temperature gradient, in a horizontal tube (Laudise *et al.*, 1998). The inner tube, in which the crystallization takes place, was cleaned and heated afterwards at T = 600 K under an Ar flow for 10 h to evaporate the solvents. The source material, with nominal 98% purity, was obtained from Sigma Aldrich. Prior to crystal growth, the powder was purified using vacuum sublimation under a temperature gradient process (Jurchescu *et al.*, 2004), designed to remove the light impurities.[2] The purified powder was placed in the hot part of the growth tube in an alumina boat. The sublimation temperature (T = 553 K) was kept as low as possible (close to the sublimation threshold). This was done to prevent the sublimation of heavy impurities and to ensure the slow sublimation rate that yields crystals with minimum structural defects. Crystals grown at slightly higher temperatures were of significantly lower quality and gave weak diffraction patterns. The growth set-up was placed in the dark to avoid oxidation. The transport gas was a mixture of H_2 (AGA, 5*N*) and Ar (AGA, 5*N*), with a volume percentage of 5.25% H_2.

The crystals are orange-colored and needle- or platelet-shaped. The typical in-plane dimensions are 200 μm × 1 cm for the needles and 3–5 mm for the platelets. The thickness of the crystals was 3–20 μm.

[1] We used the standard settings of the *International Tables for Crystallography*. The transformation to *Bbam*(*Cmca* → *Bbam*) is: $b \rightarrow a$, $c \rightarrow b$, $a \rightarrow c$. For the crystal orientation in the electronic measurements (de Boer *et al.*, 2004; Podzorov *et al.*, 2004), the *Bbam* setting was used.

[2] We refer to the species present in the system that have lower/higher molecular masses than the parent compound as 'light'/'heavy' impurities.

The single-crystal diffraction experiments were performed on a Bruker SMART APEX CCD diffractometer with graphite-monochromated Mo $K\alpha$ radiation. The crystal was cooled using a Bruker KRYOFLEX (1 h was taken to reach 100 K) and the measurements were performed during heating. Experimental details on the structure determination, data collection and refinement are summarized in Table 1 for four out of the eight temperatures reported in this work (at $T = 100$, 150, 200 K and room temperature). Information on all eight structures can be found in the CIF file accompanying this paper.[3]

3. Results and discussion

The molecule presents $2/m$ symmetry, with the asymmetric unit consisting of one quarter of a rubrene molecule. A twofold axis is located along the C1—C1*b* bond. There is a mirror plane perpendicular to the planar tetracene fragment of the molecule, through the inversion center positioned in the middle of the C1—C1*b* bond. The adopted labelling scheme and the molecular geometry are illustrated in the *ORTEP* drawings of Figs. 1(*a*)–(*d*). The plots show graphical representations of the atomic positions and their anisotropic displacement ellipsoids at four out of the eight different temperatures included in this study (T = 100, 150, 200 K and room temperature). These images provide a visual description of the vibrational motion of each atom around its equilibrium position. The crystal structure determination reveals a 2.157 (19)% volume thermal expansion of the crystal between 100 and 300 K, in agreement with the typical values measured in organic crystals. The thermal expansion is anisotropic for the three crystallographic directions [Δa = 0.410 (4)%, Δb = 0.320 (3)%, Δc = 1.562 (5)%] and occurs predominantly along the weakest bonding *c* axis (see Fig. 2).

We relate the behavior of electronic mobility *versus* temperature with structural changes. Electronic measurements performed on rubrene single crystals show that the evolution of field-effect mobility increases with decreasing temperature down to 175 K, consistent with band-like behaviour (de Boer *et al.*, 2004; Podzorov *et al.*, 2004; the results differ slightly between groups). Below 175 K the mobility drops precipitously. The dramatic decrease in the field-effect mobility can be a consequence of a structural phase transition in the material. Our diffraction experiments show that the crystallographic symmetry does not change when passing through this temperature interval. It can also be observed from Fig. 2 that the unit-cell parameters and volume are continuous with temperature. Also, the evolution of the fractional coordinates of the C atoms do not signal the presence of a phase transition. However, differential scanning calorimetry performed on the crystals exhibit the signature of a phase transition at T = 175 K. It is likely that there is a phase transition at this temperature, but it is not observed with our X-ray diffraction experiments. We will focus on this transition elsewhere (Jurchescu *et al.*, 2006).

We use the model proposed by da Silva Filho *et al.* (2005) to explain the changes in electronic properties as a response to the structural changes in the crystal. They associate the intrinsic transport properties of rubrene single crystals with the electronic coupling between adjacent molecules. The measure for this interaction is the interchain transfer integral, *t*, which varies with molecular packing. The electronic coupling is maximal if the molecules are perfectly cofacial in the crystal, oscillates when the molecular displacement increases (with positive and negative values) and becomes

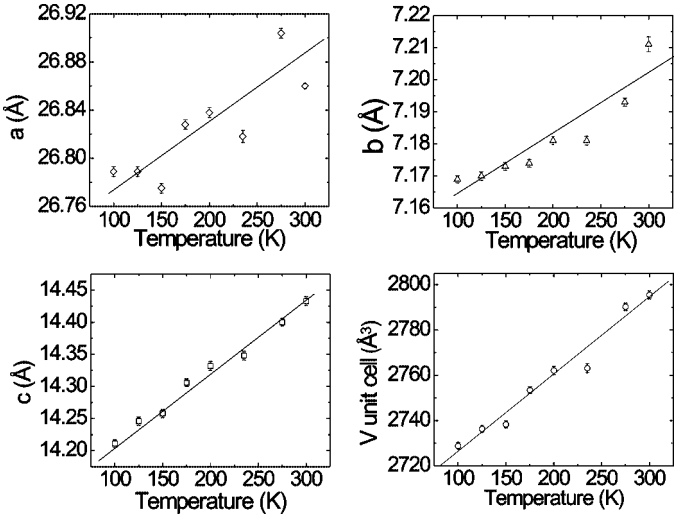

Figure 2
Lattice parameters *a*, *b* and *c*, and unit-cell volume *V versus* temperature for a rubrene single crystal. The lines are guides for the eyes.

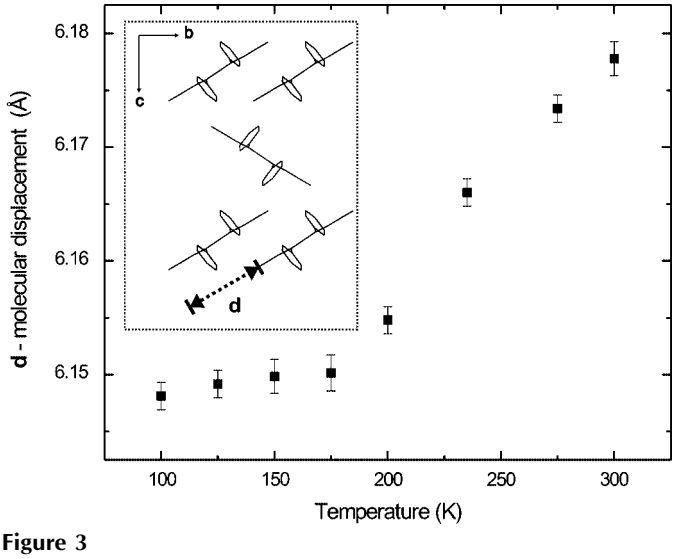

Figure 3
Evolution of the molecular displacement along the long axis of the rubrene molecule with temperature. The inset represents the rubrene molecular packing viewed along the [100] direction and defines the length *d* of the molecular displacement.

[3] Supplementary data for this paper are available from the IUCr electronic archives (Reference: BK5027). Services for accessing these data are described at the back of the journal.

zero at large shifts. This translates to the direct influence of the molecular stacking on the electronic properties.

From these calculations it is obvious that the molecular displacement, d (Fig. 3) is the relevant parameter, relating the crystal structure with the electronic mobility, similar to the model proposed by Mattheus *et al.* (2003). This parameter is complementary to molecular overlap and is given by the orientation of the tetracene backbone with respect to the crystallographic b direction. The simplified expression for d at each temperature is: $d = b \cdot \cos\Theta$, where b is the value of the unit-cell parameter (Fig. 2) and Θ is the angle that the long axis of the molecule (parallel to the C5—C5a bond) makes with the b direction.

The maximum deviation from planarity in the tetracene backbone of the molecule is for C2 and is 0.0714 (11) Å at 100 K and 0.0731 (14) Å at room temperature. The interplanar separation between two adjacent parallel molecules, along the π-stack, increases from 3.654 (3) to 3.715 (3) Å between 100 and 300 K. This length is slightly larger than the typical van der Waals interaction distance in a C—C π-stack (Bondi, 1964). The molecules slide with respect to each other along their planar part when the temperature is changed. Fig. 3 shows the temperature dependence of the molecular displacement (d) along the long axis of the molecule in a rubrene single crystal. The value of the shift increases between 100 and 300 K, as can be seen in Fig. 3. The changes of d with temperature are dominated by changes in the lattice parameter b(see Fig. 2). The variations in molecular displacement induce changes in the transfer integral (t) and determine the electronic mobility (see Fig. 4 of da Silva Filho *et al.*, 2005). The molecular displacement has a large value due to the effect of the interactions between phenyl side groups of neighboring molecules. They are arranged two by two, on different sides of the planar tetracene part of rubrene and the position is restricted by the inversion center. Their torsion with respect to the acene linear part of the molecule ranges from 80.30 (5)° at 100 K to 80.88 (7)° at room temperature. The phenyl rings positioned on the same part of the molecule make a dihedral angle of 25.32 (6)° at 100 K and 25.14 (10)° at 300 K. The connection between the phenyl rings and the tetracene fragment is the C2—C6 bond. At 100 K this bond makes an angle of 12.57 (8)° with the tetracene fragment of the molecule and 6.13 (9)° with the phenyl plane. The corresponding angles at 300 K are 12.74 (9) and 6.00 (10)°, respectively.

4. Conclusions

We conclude that rubrene single crystals grown by physical vapor transport in ambient pressure exhibit orthorombic symmetry. We see no evidence for a structural phase transition in the diffraction experiments. Further investigations concerning the mechanism that drives the dramatic changes in electronic mobility at T = 175 K in rubrene are required.

We thank I. Shokaryev for the translations from Russian journals.

References

Akopyan, S. A., Avoyan, R. L. & Struchkov, Yu. T. (1962). *Z. Strukt. Khim.* **3**, 602–605.
Boer, R. W. I. de, Gershenson, M. E., Morpurgo, A. F. & Podzorov, V. (2004). *Phys. Status Solidus A*, **201**, 1302–1331.
Bondi, A. (1964). *J. Phys. Chem.* **68**, 441–451.
Bruker (2000). *SMART*, *SAINT*, *SADABS* and *XPREP* Software Reference Manual. Bruker AXS Inc., Madison, Wisconsin, USA.
Bulgarovskaya, I., Vozzhennikov, V., Aleksandrov, S. & Belsky, V. (1983). *Latv. PSR Zinat. Akad. Vestis Fiz. Teh. Zinat. Ser.* **4**, 53–59.
Butko, V. Y., Lashley, J. C. & Ramirez, A. P. (2005). *Phys. Rev. B*, **72**, 081312.
Henn, D. E. & Williams, W. G. (1971). *J. Appl. Cryst.* **4**, 256.
Jurchescu, O. D., Baas, J. & Palstra, T. T. M. (2004). *Appl. Phys. Lett.* **84**, 3061–3063.
Jurchescu, O. D., Meetsma, A. & Palstra, T. T. M. (2006). In preparation.
Laudise, A., Kloc, C., Simpkins, P. & Siegrist, T. (1998). *J. Cryst. Growth*, **187**, 449–454.
Li, C. N., Kwong, C. Y., Djurisic, A. B., Lai, P. T., Chui, P. C., Chan, W. K. & Liu, S. Y. (2005). *Thin Solid Films*, **477**, 57–62.
Mattheus, C. C., de Wijs, G. A., de Groot, R. A. & Palstra, T. T. M. (2003). *J. Am. Chem. Soc.* **125**, 6323–6330.
Oyamada, T., Uchiuzou, H., Akiyama, S., Oku, Y., Shimoji, N., Matsushige, K., Sasabe, H. & Adachi, C. (2005). *J. Appl. Phys.* **98**, 074506.
Podzorov, V., Menard, E., Borissov, A., Kiryukhin, V., Rogers, J. A. & Gershenson, M. E. (2004). *Phys. Rev. Lett.* **93**, 086602.
Sheldrick, G. M. (1997*a*). *SHELXS*97. University of Göttingen, Germany.
Sheldrick, G. M. (1997*b*). *SHELXL*97. University of Göttingen, Germany.
Silva Filho, D. A. da, Kim, E. G. & Bredas, J. L. (2005). *Adv. Mater.* **17**, 1072–1076.
Spek, A. L. (2003). *J. Appl. Cryst.* **36**, 7–13.
Sundar, V. C., Zaumseil, J., Podzorov, V., Menard, E., Willett, R. L., Someya, T., Gershenson, M. E. & Rogers, J. A. (2004). *Science*, **303**, 1644–1646.
Taylor, W. H. (1936). *Z. Kristallogr.* **93**, 151–155.